


## ORIGINAL ARTICLE

# A novel tumor suppressor role of myosin light chain kinase splice variants through downregulation of the TEAD4/CD44 axis

Yen-Ju Huang<sup>1</sup>, Tsung-Chun Lee<sup>1,2</sup>, Yu-Chen Pai<sup>1</sup>, Been-Ren Lin<sup>3</sup>, Jerrold R. Turner<sup>4</sup> and Linda Chia-Hui Yu<sup>1,\*</sup>,

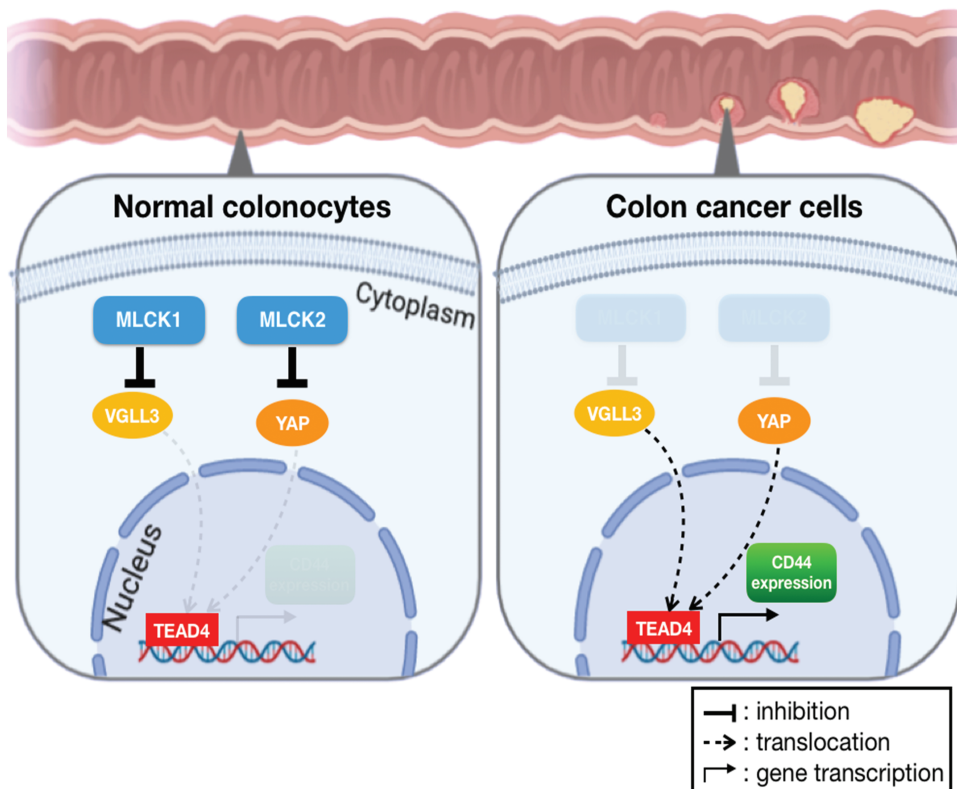
<sup>1</sup>Graduate Institute of Physiology, National Taiwan University College of Medicine, Taipei, Taiwan ROC, <sup>2</sup>Department of Internal Medicine, National Taiwan University Hospital and College of Medicine, Taipei, Taiwan ROC, <sup>3</sup>Department of Surgery, National Taiwan University Hospital and College of Medicine, Taipei, Taiwan ROC and <sup>4</sup>Brigham's Women Hospital, Harvard Medical School, Boston, MA, USA

\*To whom correspondence should be addressed. Tel: 886-2-23123456 ext. 88237; Fax: 886-2-23964350; Email: [lchyu@ntu.edu.tw](mailto:lchyu@ntu.edu.tw)

## Abstract

Myosin light chain kinase (MLCK) regulates actinomyosin contraction. Two splice variants of long MLCK are expressed in epithelial cells and divergently regulate gut barrier functions; reduced MLCK levels in human colorectal cancers (CRC) with unclarified significance have been reported. CRC are solid tumors clonally sustained by stem cells highly expressing CD44 and CD133. The aim was to investigate the role of MLCK splice variants in CRC tumorigenesis. We found lower MLCK1/2 and higher CD44 expression in human CRC, but no change in CD133 or LGR5. Large-scale bioinformatics showed an inverse relationship between MYLK and CD44 in human sample gene datasets. A 3-fold increased tumor burden was observed in MLCK(-/-) mice compared with wild-type (WT) mice in a chemical-induced CRC model. Primary tumorspheres derived from the MLCK(-/-) mice displayed larger sizes and higher CD44 transcript levels than those from the WT mice. Bioinformatics revealed binding of TEAD4 (a transcriptional enhancer factor family member in the Hippo pathway) to CD44 promoter, which was confirmed by luciferase reporter assay. Individually expressing MLCK1 and MLCK2 variants in the MLCK-knockout (KO) Caco-2 cells inhibited the nuclear localization of TEAD4 cofactors, VGLL3 and YAP1, respectively, and both variants reduced the CD44 transcription. Accelerated cell cycle transit was observed in the MLCK-KO cells, whereby expression of MLCK1/2 variants counterbalanced the cell hyperproliferation. In conclusion, MLCK1/2 variants are novel tumor suppressors by downregulating the TEAD4/CD44 axis via reducing nuclear translocation of distinct transcriptional coactivators. The reduction of epithelial MLCKs, especially isoform 2, may drive cancer stemness and tumorigenesis.

## Graphical Abstract



## Abbreviations

CRC,	colorectal cancers
CSC,	cancer stem cells
GTRD,	Gene Transcription Regulation Database
KO,	knockout
LGR,	leucine-rich repeat-containing G-protein-coupled receptor
MLC,	myosin light chain
MLCK,	Myosin light chain kinase
TAZ,	transcriptional coactivator with PDZ-binding motif
TCGA,	The Cancer Genome Atlas Program
TEAD4,	transcriptional enhanced associate domain 4
VGLL3,	Vestigial-like 3
WT,	wild-type
YAP,	yes-associated protein.

## Introduction

Myosin light chain kinase (MLCK) is a calcium/calmodulin-dependent serine-threonine kinase that phosphorylates myosin light chain (MLC) to enable actinomyosin contraction in muscle and non-muscle cells. The human MLCK is comprised of short (130 kD) and long (210 kD) isoforms encoded by different transcriptional promoters of a single *MYLK* gene (1). The short form of MLCK was originally identified in muscle cells, and the long form of MLCK was found in epithelial cells. Intestinal epithelial cells constitutively express two splice variants of long

MLCK for the regulation of barrier functions; the full-length MLCK1 differs from MLCK2 by a single exon (207 bp) encoding for 69 amino acids (2,3). The activation of MLCK1 regulates paracellular junctional opening (2,4), whereas MLCK2 accounts for terminal web contraction and brush border fanning which increases transcellular permeability (5,6). While the physiological function of long MLCKs in intestinal epithelia is well established, the roles of long MLCKs in the tumorigenesis of colorectal cancers (CRC) remain controversial.

Colorectal carcinoma is ranked the second cause of cancer death globally and is derived from malignant epithelial cells (7). Decreased MLCK transcripts with unknown pathological significance have been reported in human CRC specimens (8,9). Opposing results on the role of MLCK in tumorigenesis were documented in experimental models. Pharmacological blockade of MLCK reduced the growth of colorectal, breast and prostate tumors in rodent models (10,11). Other studies showed that MLCK is involved in spindle assembly during cell division, and inhibition of MLCK in non-malignant cells causes multinucleation and multipolar spindles, which are similar to cancer cell phenotypes with mitotic defects (12,13). Previous work in late-stage colon cancer and liver cancer cells showed that cell migration and epithelial-mesenchymal transition were dependent on MLCK activities (14-16). Furthermore, a transcribed *MYLK* pseudogene (*MYLKP*) was recently documented to be highly expressed in colon and lung tumor cells and may inhibit *MYLK* gene expression and promote cell proliferation (9,17). To date, the mechanistic details of MLCK involvement in colon carcinogenesis remain poorly understood.

Unlimited proliferation and dysregulated stemness are the major hallmarks of cancer. A growing body of evidence

suggested that cancer stem cells (CSC) played a key role in the progression of neoplasia (18,19). While leucine-rich repeat-containing G-protein-coupled receptor (LGR5)-positive stem cells are found in normal intestinal crypts, CSCs isolated from colon cancers show high expression of CD44 and CD133 molecules and are capable of forming increased numbers and larger sizes of tumorspheres *in vitro* (20–22). The cell population highly expressed with CD44/CD133 cell population can develop into heterogeneous tumors with hyperproliferative potency when transplanted into immunodeficient mice (23,24). Moreover, the CD44 standard form and splicing variants act as growth factor coreceptors to promote epithelial and tumor cell proliferation (25–27). Whether dysregulated stemness is involved in MLCK-dependent cancer progression has yet to be explored.

In the present study, the role of long MLCK in the regulation of cancer stemness and tumor cell proliferation was investigated using human CRC specimens, genetically modified mice, primary tumor spheroids and gene knockout (KO) cell lines. Our results demonstrated that MLCK1/2 splice variants regulated distinct coactivators to interact with the novel transcription factor TEAD4 for CD44 promoter activity.

## Materials and methods

### Human surgical specimens

Surgical specimens of paired tumor and adjacent non-tumor tissues from 20 patients with CRC were collected in National Taiwan University Hospital (NTUH) (Supplementary Table 1, available at *Carcinogenesis* Online). Written informed consent was obtained from all study subjects, and the approval for this study was granted by the Research Ethics Committee of NTUH (200912049R).

### Polymerase chain reaction (PCR)

Quantitative PCR was performed using primer pairs designed in this study based on the NCBI nucleotide sequence of each gene (Supplementary Tables 2 and 3, available at *Carcinogenesis* Online). Gene expression was calculated from the difference of the threshold cycle (Ct) between the target gene and endogenous housekeeping gene as  $\Delta$ Ct. The relative gene expression is expressed as the fold difference ( $2^{-\Delta\Delta Ct}$ ). Alternatively, semiquantitative PCR was performed using primer pairs (Supplementary Table 4, available at *Carcinogenesis* Online) (6,28).

### Data mining and bioinformatics analysis

The Gene Transcription Regulation Database (GTRD, <http://gtrd.biouml.org>) based on chromatin immunoprecipitation results was applied for prediction of transcription factor binding sites close to the human CD44 gene (Chromosome 11, 35138870–35232402). The RNA-seq-based gene expression datasets were generated by The Cancer Genome Atlas Program (TCGA) Research Network (<http://cancergenome.nih.gov>) and downloaded from the cBioPortal and Xena computational programs. Overall, the MYLK, CD44 and other mRNA expression levels in 1672 samples from 5 studies were retrieved for cBioPortal analysis. A TCGA TARGET GTEx of the colon-specific dataset of 639 samples was generated by the Xena program from University of California, Santa Cruz.

### Animals

Specific pathogen-free wild-type (WT) C57BL/6 male mice were obtained from the Animal Center of National Taiwan University College of Medicine (NTUCM). Mice deficient of long 210 kD MLCK [MLCK(–/–)] on a B6 background were obtained from the Turner laboratory (5). All experimental procedures were approved by the Animal Care and Use Committee of the National Taiwan University.

### Reagents

Pharmacological inhibitors include ML-7 (a MLCK inhibitor targeting the ATPase domain) and verteporfin (a specific inhibitor to TEAD activation) were bought from Sigma-Aldrich. A membrane-permeant inhibitor of

MLCK PIK (Dreverse PIK, a specific MLCK inhibitor targeting the kinase domain) is a gift from the Turner laboratory (29).

### Mouse model of chemical-induced CRC

The WT B6 and MLCK(–/–) mice were subjected to colon cancer induction according to previously established methods (30,31). Briefly, mice were injected intraperitoneally (i.p.) with a mutagen azoxymethane (AOM) (10 mg/kg body wt), and after 7 days, given 2% dextran sodium sulfate (DSS) in drinking water for 4 days, followed by 3 days of regular water. This cycle of AOM/DSS was performed 3 times, and animals were euthanized on days 84 and 126 to determine tumor burden. Tumor tissues were developed into primary spheroid cultures for experiments (30,31).

### Primary mouse colonic organoid and tumor spheroid cultures

Colonic tumors were cultured as spheroids and colonic organoids were developed from intestinal crypts following previously described methods (30,31). A total number of 80–100 spheroids or organoids per group were quantified for area by using imaging software (AxioVision, Zeiss).

### Human CRC cell lines

Human Caco-2 cells (clone C2BBE) and HT-29 (ATCC HTB-38) were grown in DMEM supplemented with 10% FBS and penicillin/streptomycin (Sigma-Aldrich) (28,32,33). The cells were authenticated by STR profile analysis in the Biosource Collection and Research Center in Taiwan.

### Gene KO using the CRISPR/Cas9 gene editing system

The KO of the MYLK gene (Gene ID: 4638) in Caco-2 cells was conducted using Clustered Regularly Interspaced Short Palindromic Repeats/CRISPR-associated protein 9 (CRISPR/Cas9) technique at the First Research Core Laboratory of NTUCM. The CRISPR RNA (crRNA) including CR-1 and CR-2 which targeted two sites of human MYLK gene are 5'-CCTGGGAACCGG AGTGTGTTGTCT-3' and 5'-CCACCGCCAAGTTCGAAGGGCGG-3', respectively. For gene expression in the KO cells, plasmids carrying the MLCK1 (GenBank: NM\_053025.4) or MLCK2 (GenBank: NM\_053026.4) sequence were transfected into the KO cells prior to the experiments of real-time PCR and flow cytometry analysis.

### Gene knockdown by transduction with lentiviral delivery of short hairpin RNA (shRNA)

The lentivirus containing shRNA was assembled from shRNA oligonucleotides targeting MYLK gene in a modified pLKO.1-puromycin vector, packaging plasmids (pCMV-R8.74psPAX2) and envelope plasmids (pMD2.G). For the shRNA-mediated gene knockdown experiment, Caco-2 cells seeded for 1 day were infected with the lentiviral medium mixed with culture medium at a ratio of 1:1 with 8  $\mu$ g/ml polybrene for 2 days and then selected by culturing in medium containing 8  $\mu$ g/ml puromycin for 48 h.

### Luciferase reporter assay

The expression vector pcDNA3.1 carrying the human TEAD4 sequence (Gene ID: 7004) and the luciferase reporter vector pGL3-Basic vector with the human CD44 promoter (–1880 to +133) (Gene ID: 960) were constructed. HEK293T cells were seeded into 24-well plates at a concentration of  $1 \times 10^5$  cells per well for 16 h. Cells were transfected with plasmid pGL3-hCD44 promoter-Luc and pGL4.74-hRluc in a 37°C incubator for 24 or 48 h. The cell lysate was centrifuged, and the resultant supernatant was analyzed using a Dual-Glo™ Luciferase assay system (Promega, Madison, WI). A microplate luminometer was utilized to detect firefly luciferase activity and Renilla luciferase activity. The induction value of firefly/Renilla indicated the normalized promoter activity.

### Western blotting

Proteins were extracted with complete radioimmunoprecipitation assay buffer and subjected to gel electrophoresis as previously described (32,34). The primary antibodies used included mouse anti-human MLCK [#sc-365352, clone: MYLK (A-8)] (1:1000, Santa Cruz), mouse anti-human CD44

[#sc-9960, clone: HCAM (F-4)] (1:500, Santa Cruz), mouse anti-human TEAD4 [#sc-390578, clone: TEF (B-5)] (1:1000, Santa Cruz), rabbit anti-human YAP1 (#4912) (1:1000, Cell Signaling), rabbit anti-human VGLL3 (#AB83555) (1:500, Abcam) and anti- $\beta$ -actin (1:10000, Sigma-Aldrich). The secondary antibodies used were horseradish peroxidase-conjugated horse anti-mouse IgG and goat anti-rabbit IgG. The membranes were incubated with chemiluminescent solution and signals detected for the determination of band density.

### Cell cycle analysis by flow cytometry

Caco-2 cells stained with anti-Ki67 and propidium iodide were used for cell cycle analysis as described (28). A minimum of 10 000 propidium iodide-stained nuclei were analyzed, and the percentages of cells in the  $G_0$ - $G_1$ , S and  $G_2$ -M phases of the cell cycle and the ratio of cells with high-to-low intensity of Ki67 were determined using FlowJo cell cycle analysis software v.7.6.1 (BD Biosciences).

### Statistical analysis

All data are presented as mean  $\pm$  standard error of the mean (SEM), and dot plots were added for clarification. Unpaired t-test with Welch's test is adopted when the two groups of samples are unpaired and are normally distributed (GraphPad Prism version 6). The paired tumor and non-tumor tissues of patients were compared using paired t-test and non-parametric Wilcoxon matched-pairs signed-rank test. When more than three groups were compared, the one-way analysis of variance (ANOVA) was chosen to examine differences between groups and a Tukey multiple comparison test was selected as a post-hoc test to determine the P-value. A value of  $P < 0.05$  was considered statistically different. Detailed methods are described in the [Supplementary Material and Methods](#), available at [Carcinogenesis Online](#).

## Results

### Decreased MLCK transcripts associated with increased CD44 expression in human tumor specimens

Surgical specimens of human CRC and paired non-tumor tissues from 20 patients ([Supplementary Table 1](#), available at [Carcinogenesis Online](#)) were analyzed for the relative expression of long MLCK and stem cell markers, such as CD44, CD133 and LGR5. Quantitative PCR results revealed lower MLCK transcripts, including both splice variants MLCK1 and MLCK2 encoded by a single MYLK gene, in tumor specimens compared with the paired adjacent non-tumor tissues ([Figure 1A](#)). No difference in the MYLK was observed between the tumor and non-tumor tissues ([Figure 1B](#)). Moreover, higher CD44 levels, including the standard and variant forms, were observed in the tumor tissues, whereas the CD133 and LGR5 transcript levels were not different between the tumor and non-tumor groups ([Figure 1C-E](#)).

Previously reported transcription factors for CD44, e.g. SP1, TP63 and TP53 (35-37) and novel candidates, such as transcriptional enhanced associate domain 4 (TEAD4), were also assessed in the paired tumor and non-tumor tissues. The gene sequence of TEAD4 was aligned to the CD44 promoter based on the GTRD. Significant differences in abundance between the tumor and non-tumor tissue were observed in the SP1, TP63, TP53 and TEAD4 transcripts ([Figure 1F](#)).

We further evaluated the altered gene expression of MYLK in correlation with CD44 and its potential transcriptional factors using datasets in TCGA Research Network. Approximately 5% of CRC patients displayed MYLK gene mutations according to a cBioPortal analysis with 1672 samples from five studies ([Figure 2A](#)). The expression of MYLK decreased, whereas CD44 increased

in advanced CRC tissues compared with normal tissues based on the Xena program with TCGA TARGET GTEx of the colon-specific cohort (639 matching samples) ([Figure 2B](#)). Moreover, the heatmap of MYLK mRNA in CRC samples was opposite to that of TP53 and TEAD4 ([Figure 2C](#)). The changes in SP1 and TP63 were not correlated with CD44 expression. Among the candidate transcription factors, TP53 and TEAD4 showed a similar trend to CD44, which was inversely correlated with MLCK expression. The co-occurrence of MYLK with CD44 and its candidate transcription factors (SP1, TP63 and TEAD4) was revealed by cBioPortal analysis in 1672 samples, whereas mutual exclusivity of MYLK with TP53 was shown ([Figure 2D](#)). Therefore, TEAD4 was chosen as a potential candidate transcriptional factor for MLCK-dependent regulation of CD44 expression.

### Higher tumor burden with elevated CD44 expression in mice deficient of long MLCK

Mice deficient in long 210 kD MLCK [MLCK(-/-)] and WT C57BL/6 (B6) mice were compared for tumor growth using a chemical-induced colon cancer model. The absence of the long MLCK transcript was first confirmed by PCR on mucosal tissues of untreated MLCK(-/-) mice ([Supplementary Figure 1A](#), available at [Carcinogenesis Online](#)). A 2- to 3-fold higher tumor number and area were observed in the MLCK(-/-) mice than in the WT mice ([Figure 3A and B](#)). Low-grade (11%) and high-grade (55.6%) dysplasia and carcinoma (33.3%) were observed in the B6 tumors, whereas high-grade dysplasia (62.5%) and carcinoma (37.5%) were found in the MLCK(-/-) tumors.

Primary spheroid cultures were developed from the tumor tissues of the MLCK(-/-) and B6 mice to evaluate the expression of cancer stemness markers. Increased tumorsphere size and proliferating cell nuclear antigen levels were found in those derived from the MLCK(-/-) mice compared with those from the WT mice ([Figure 3C-E](#)). Higher CD44 expression was observed in the tumorspheres derived from the MLCK(-/-) mice than the WT mice ([Figure 3F](#)). In contrast, no difference of the CD133 or LGR5 levels in the tumorspheres was found between the two mouse groups ([Figure 3F](#)). A trend of increase in TEAD4 expression without statistical significance was seen in the MLCK(-/-) tumorspheres ([Figure 3F](#)). Immunofluorescent staining showed that CD44 protein was not homogeneously distributed in the mouse tumor tissues. Although higher CD44 immunoreactivity was observed in some areas of the MLCK(-/-) tumors than those of B6 tumors, the patchy distribution of CD44 staining rendered it difficult to be quantified ([Figure 3G](#)).

### An inhibitory role of MLCK in epithelial proliferation and tumor growth

To rule out the possibility that tumor microenvironment *in vivo* affects the primary spheroid sizes, we subjected the WT B6 tumorspheres to pharmacological inhibition or gene knockdown to validate the direct role of the MLCK in tumor growth. Pretreatment with ML-7 or gene silencing of MYLK led to increased growth of B6 tumorspheres *in vitro* ([Figure 4A and B](#)). The knockdown efficiency of MYLK was shown in [Figure 4C](#). In addition, primary colonic organoids derived from the untreated MLCK(-/-) mice and B6 mice were also assessed to determine the involvement of MLCK in intestinal epithelial proliferation. Larger organoid areas were found in those derived from the MLCK(-/-) than those from the B6 mice ([Figure 4D](#)). Increased CD44, CD133, LGR5 and TEAD4 levels were noted in the MLCK(-/-) colonic organoids ([Figure 4E](#)), suggesting that MLCK-dependent

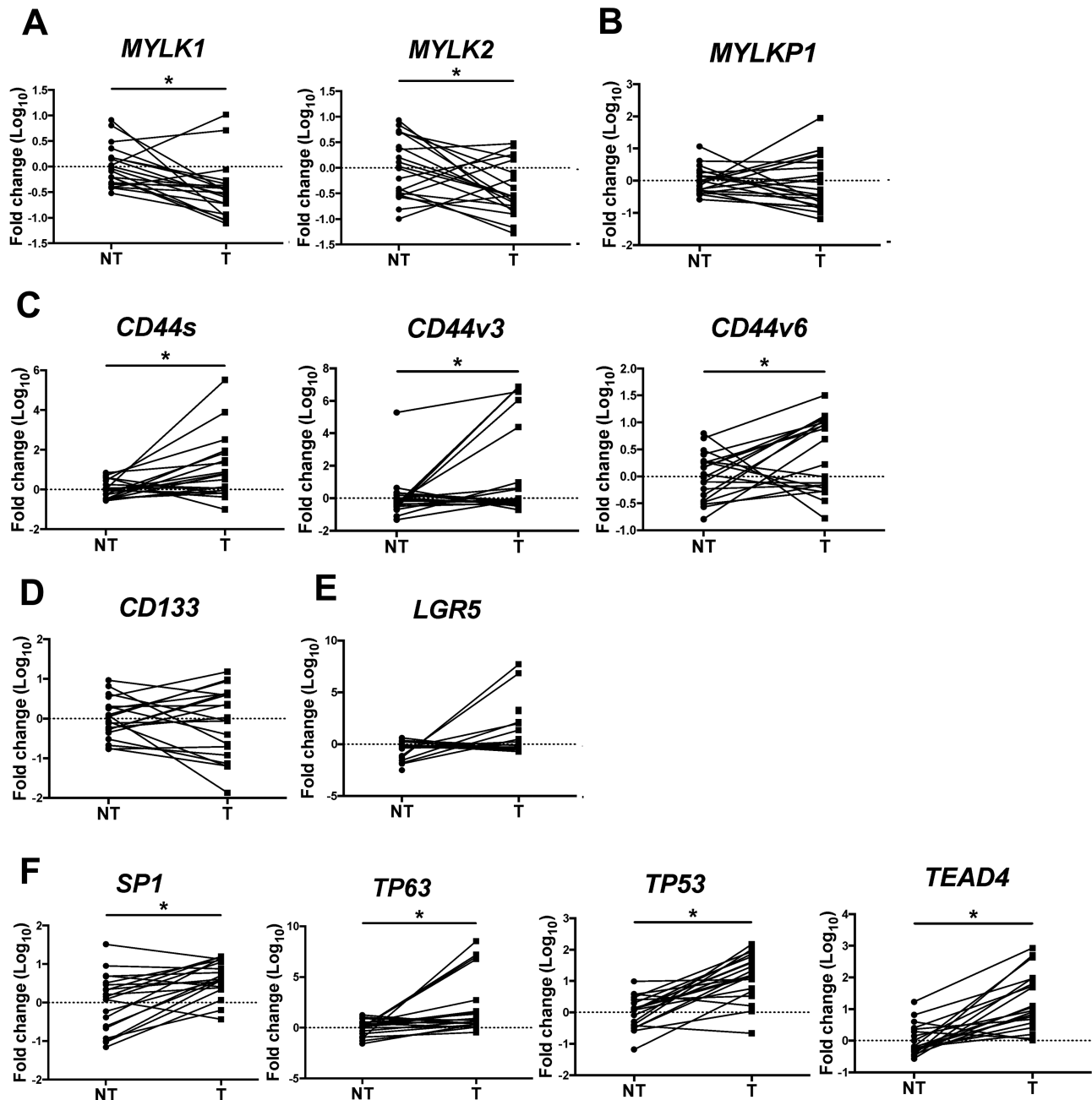


**Figure 1.** Decreased *MYLK* transcript was associated with increased stemness marker *CD44* but not *CD133* or *LGR5* in human CRC specimens. Quantitative PCR results showing the relative expression of (A) long *MYLK* splice variants *MLCK1/2* encoded by a single *MYLK* gene in paired tumor (T) and adjacent non-tumor (NT) tissues. \* $P < 0.05$ ;  $N = 20$ /group. Each dot represents the data of one patient. (B) The relative expression of *MYLK1*, (C) *CD44* including the standard form (*CD44s*), variant form 3 (*CD44v3*) and variant form 6 (*CD44v6*), (D) *CD133*, (E) *LGR5*, in paired T and NT tissues. (F) Expression of the putative and predicted transcription factors for *CD44* promoter such as *SP1*, *TP63*, *TP53* and *TEAD4*, in tumor specimens. \* $P < 0.05$ ;  $N = 20$ /group. In addition to the previously reported transcription factors (i.e. *SP1*, *TP63* and *TP53*), a novel molecule *TEAD4* was predicted for binding to the *CD44* promoter site based on GTRD analysis.

stemness repression may occur in normal colonic epithelial cells prior to malignant transformation. Normal morphology of colonic tissues was observed in the *MLCK(-/-)* mice and B6 mice prior to carcinogen administration (Supplementary Figure 1B, available at [Carcinogenesis Online](#)).

#### **MLCK suppressed *CD44* expression through regulation of *TEAD4* transcriptional activity**

Human colorectal carcinoma Caco-2 cells were pretreated with ML-7 and PIK (*MLCK* inhibitors) prior to measurement of stem cell markers. Increased *CD44* expression was

observed following ML-7 or PIK treatment in cells (Figure 5A and B). Moreover, knockdown of *MYLK* gene by shRNA also increased *CD44* but not the *CD133* or *LGR5* transcripts in Caco-2 cells (Figure 5C). The transcription factors involved in *MLCK*-dependent *CD44* suppression were then investigated. Knockdown of *MLCK* resulted in increased *TEAD4* expression in Caco-2 cells, without changes in *SP1*, *TP63* and *TP53* (Figure 5D). Western blots showed the reduction of *MLCK* protein levels associated with augmentation in *CD44* protein and a trend of increase in *TEAD4* protein following gene silencing of *MYLK* (Figure 5E).

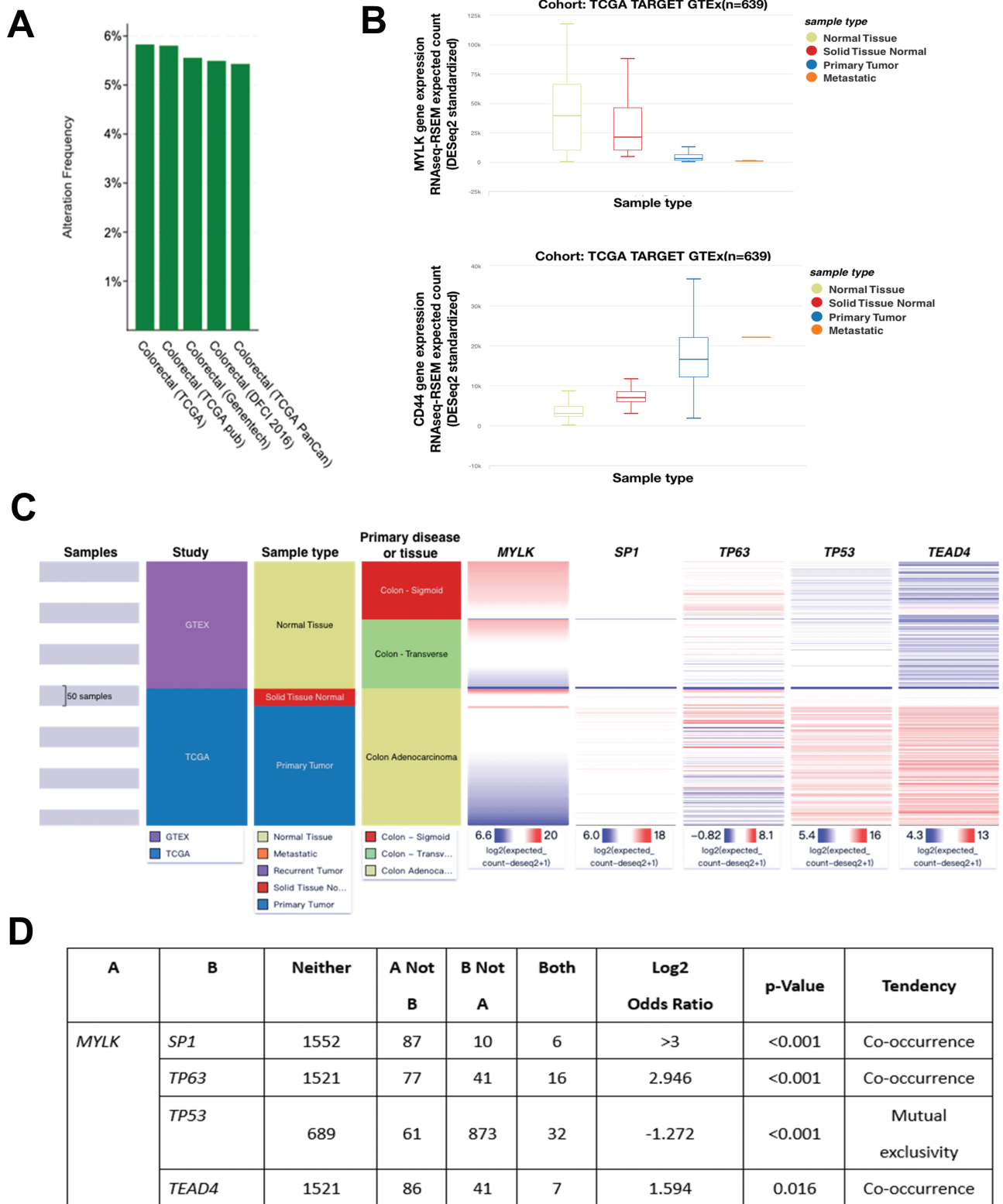


**Figure 2.** Bioinformatic analysis confirmed an inverse relationship between MYLK and CD44 in gene expression datasets of human samples. The altered gene expression of MYLK in correlation to CD44 and its candidate transcriptional factors (i.e. SP1, TP63, TP53 and TEAD4) were further examined by large-scale bioinformatics. (A) The percentage of MYLK gene mutation is approximately 5% of CRC patients based on cBioPortal analysis from The Cancer Genome Atlas (TCGA) datasets of 1672 samples. (B) The expression of MYLK decreases, whereas CD44 increases in advanced CRC tissues compared with normal tissues based on a Xena program with TCGA TARGET GTEx of colon-specific cohort (639 matching samples). Higher levels of MYLK were found in normal tissues and adjacent non-tumor tissues, whereas higher levels of CD44 were noted in primary and metastatic tumors. The gene expression is presented by RNA-seq expected count (DESeq2 standard). Statistical significance ( $P < 0.001$ ) among groups was established by ANOVA. (C) The Xena analysis depicted an inverse correlation of MYLK gene with TP53 and TEAD4, showing a similar trend to CD44 expression. The changes in SP1 and TP63 did not correlate well with the CD44 expression. (D) The cBioPortal analysis of MYLK with candidate transcription factors to CD44 promoters in TCGA datasets of 1672 patients. The Log<sub>2</sub> odds ratio is to quantify how strongly the presence or absence of alterations in A is associated with alterations in B in the selected samples. Odds ratio = (neither × both)/(A not B × B not A). The ratio > 0 indicates a tendency toward co-occurrence; the ratio ≤ 0 indicates a tendency toward mutual exclusivity.

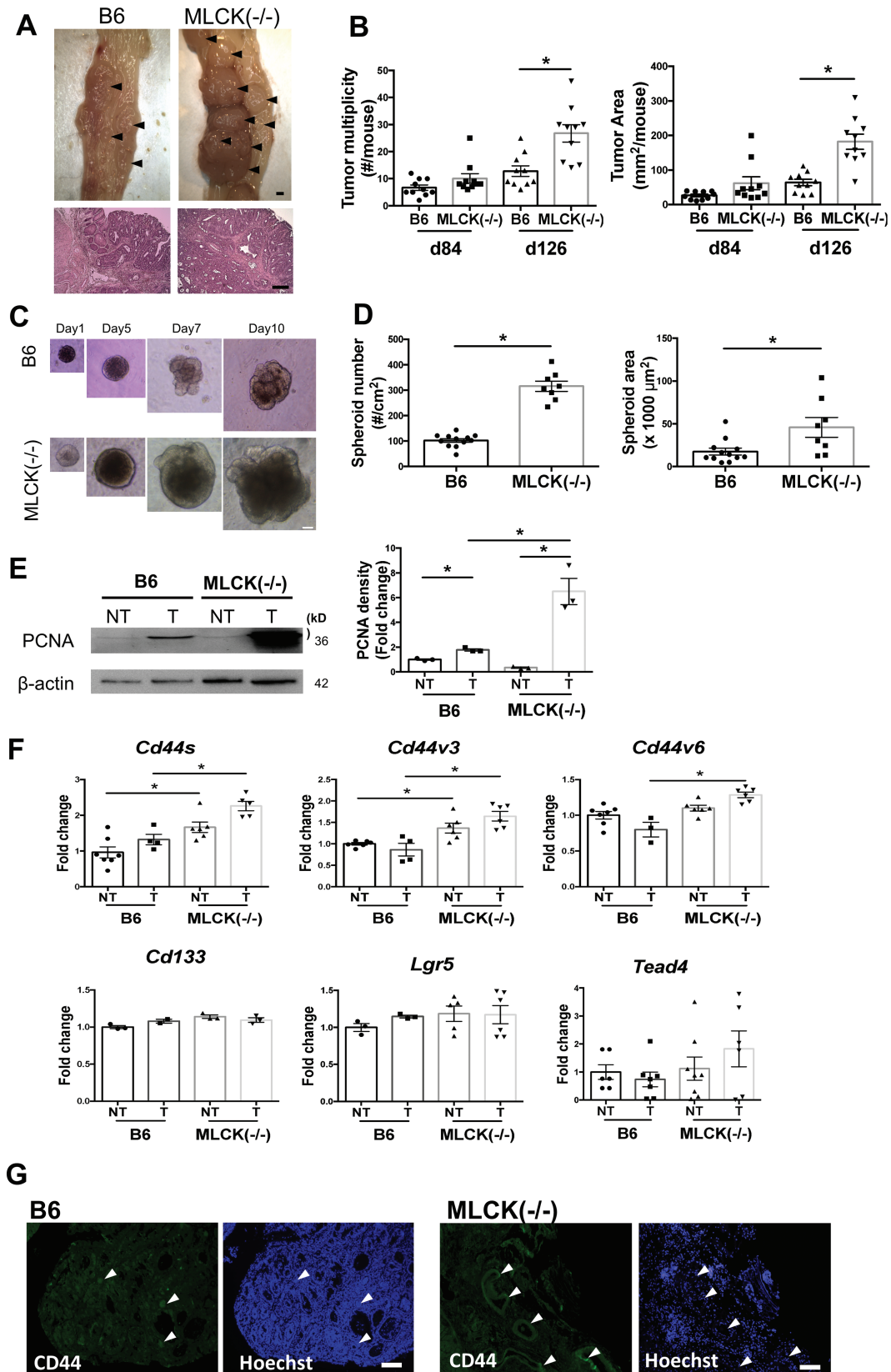


**Figure 3.** Increased tumor burden was accompanied by higher *CD44* expression in *MLCK(-/-)* mice compared with WT mice in chemical-induced CRC models. WT B6 and *MLCK(-/-)* mice were administered carcinogen for induction of colorectal tumors for 84 or 126 days. (A) Representative macroscopic images of distal colon (Bar: 1 mm) and histopathological images of colonic tumors on day 126 (Bar: 100 μm). (B) Tumor multiplicity and area on days 84 and 126. \**P* < 0.05. *N* = 10/group. Each dot represents the data of one mouse. (C) Photoimages of primary tumor spheroids derived from B6 and *MLCK(-/-)* mice for culturing of 1, 5, 7 and 10 days. Bar: 50 μm. (D) The number and area of tumor spheroids. The colony numbers grown for 5 days were determined from 20 wells per group. The average area of 150–200 tumorspheres was calculated. (E) Western blots of proliferating cell nuclear antigen (PCNA) in spheroids derived from non-tumor (NT) and tumor (T) tissues. \**P* < 0.05 versus NT; #*P* < 0.05 versus B6. (F) Expression of stemness markers in tumor spheroids, such as *CD44*, *CD133* and *LGR5*. \**P* < 0.05. *N* = 6/group. (G) Representative immunofluorescent images showing *CD44* staining (green color, arrows) in mouse tumor tissues. Cell nuclei were stained with a Hoechst dye (blue color, arrows) for tissue orientation. Bar: 100 μm. *N* = 3/group.

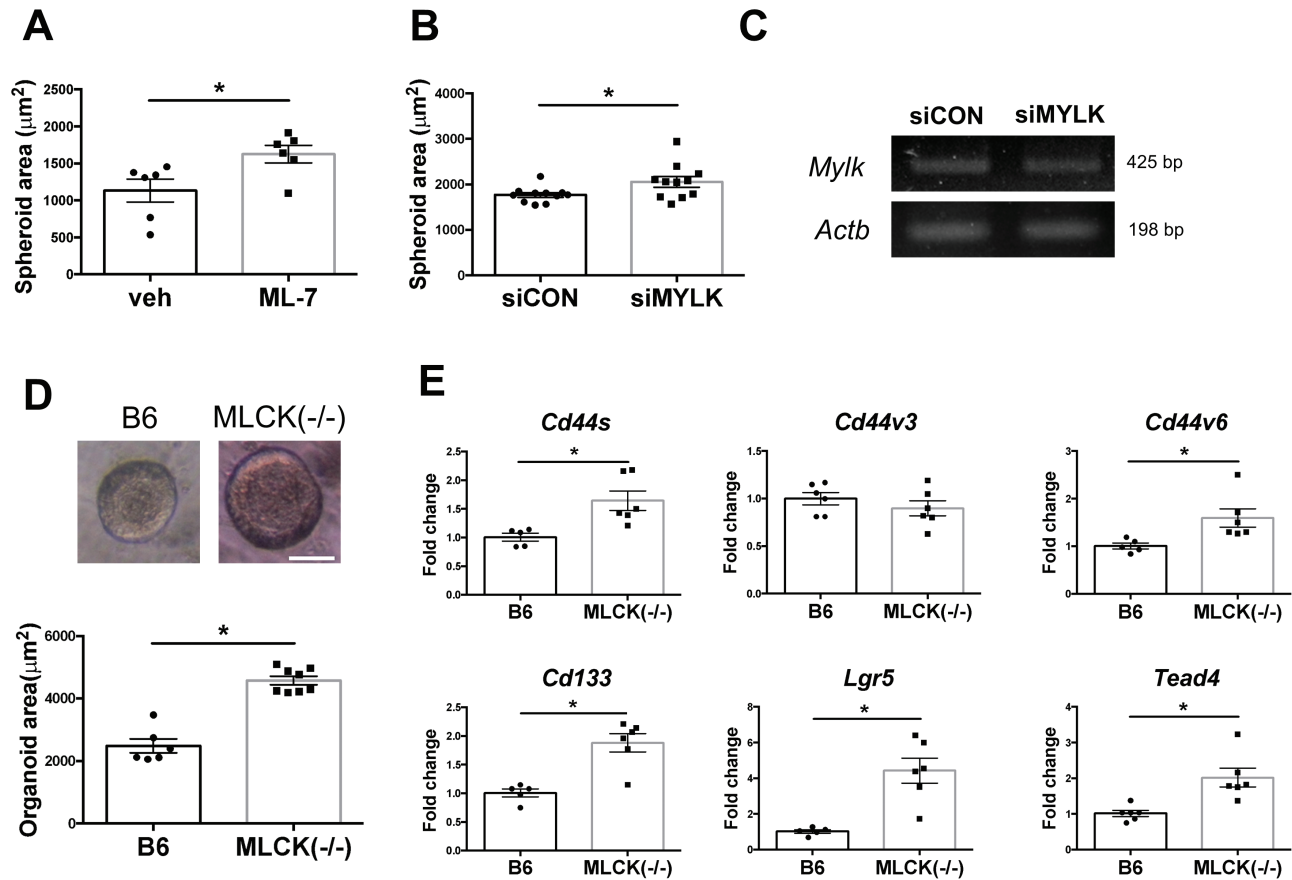


**Figure 4.** Inhibition of MLCK enhanced the growth of WT mouse tumorspheres. Spheroid cultures derived from WT B6 mouse tumors were grown for 4 days and treated with ML-7 (20 µM, an MLCK inhibitor) or gene silenced with small interfering (si)RNA for 96 h in vitro. (A) Increased area of WT tumorspheres by ML-7. \**P* < 0.05 versus vehicle. *N* = 6/group. (B) Increased area of WT tumorspheres by siMYLK. \**P* < 0.05 versus siCON. *N* = 11/group. (C) Knockdown efficiency of siMYLK was shown by reduced levels of MYLK expression. (D) Photoimages showing the size of primary organoid cultures derived from colonic crypts of untreated WT B6 and MLCK(-/-) mice. Bar: 50 µm. The average area of 180–200 colonic organoids grown for 7 days was calculated. (E) Increased expression of CD44, CD133, LGR5 and TEAD4 was observed in the MLCK(-/-) colonic organoids. \**P* < 0.05 versus B6. *N* = 6/group.

Based on the bioinformatics prediction of the aligned sequence of TEAD4 by GTRD, the binding of TEAD4 on the CD44 promoter was validated by using a luciferase reporter assay (Figure 5F). Furthermore, blockade of TEAD4 transcriptional activity by treatment with verteporfin attenuated the CD44 expression in two human CRC cell lines (Figure 5G). The TEADs are key transcription factors in the Hippo pathway regulated by the cofactor yes-associated protein (YAP) for growth control, whereas hyperactivation of YAP was associated with CRC (38,39). A Hippo-independent regulator Vestigial-like 3 (VGLL3) was identified to either compete or work in concert with YAP for TEAD4 activity (40,41), and VGLL3 expression promoted tumor proliferation (42). Therefore, the individual roles of MLCK splice variants on the nuclear localization of Hippo-dependent or -independent transcriptional cofactors and the regulation of cell proliferation were next investigated.

#### Divergent regulation of the TEAD4 transcriptional cofactors VGLL3 and YAP1 by MLCK1 and MLCK2 splice variants

To distinguish the individual role of each splice variant, we subjected WT Caco-2 cells to CRISPR/Casp-9-based KO of the MYLK gene and then transfected them with plasmids encoding MLCK1/2 sequences. The presence and absence of MLCK in WT

and KO cells was confirmed by quantitative PCR, western blotting and gene sequencing (Figure 5H; Supplementary Figure 2, available at Carcinogenesis Online). Lower expression of CD44 but not CD133 or LGR5 was observed in the KO cells individually expressing MLCK1 and MLCK2 (Figure 5I). In addition, WT Caco-2 cells overexpressing the splice variants MLCK1 and MLCK2 by plasmid transfection also exhibited reduction in CD44 expression but no change in the CD133 or LGR5 levels (Supplementary Figure 2, available at Carcinogenesis Online).

The nuclear translocation of the transcriptional cofactors was evaluated in the WT and KO cells. Western blots showed the presence of the YAP1 and VGLL3 proteins in the cytoplasmic and nuclear fractions, whereas TEAD4 was observed only in the nucleus of the WT and KO cells (Figure 5J). Densitometric analysis showed a significant increase in YAP1 but no change in VGLL3 levels in the nuclear fractions of KO cells compared with the WT cells (Figure 5K). In contrast, no difference in the cytoplasmic YAP1 or VGLL3 levels was observed between the WT and KO cells (Figure 5K). Moreover, the KO cells transfected with plasmids encoding human MLCK1 or MLCK2 showed a decrease in the nuclear VGLL3 and YAP1 levels, respectively (Figure 5K).

The presence of TEAD4 was found exclusively in the cell nuclei of WT and KO cells by immunofluorescent staining (Figure 6A). The nuclear presence of YAP1 was more evident in the KO cells compared with WT cells (Figure 6A; Supplementary Figure 3,



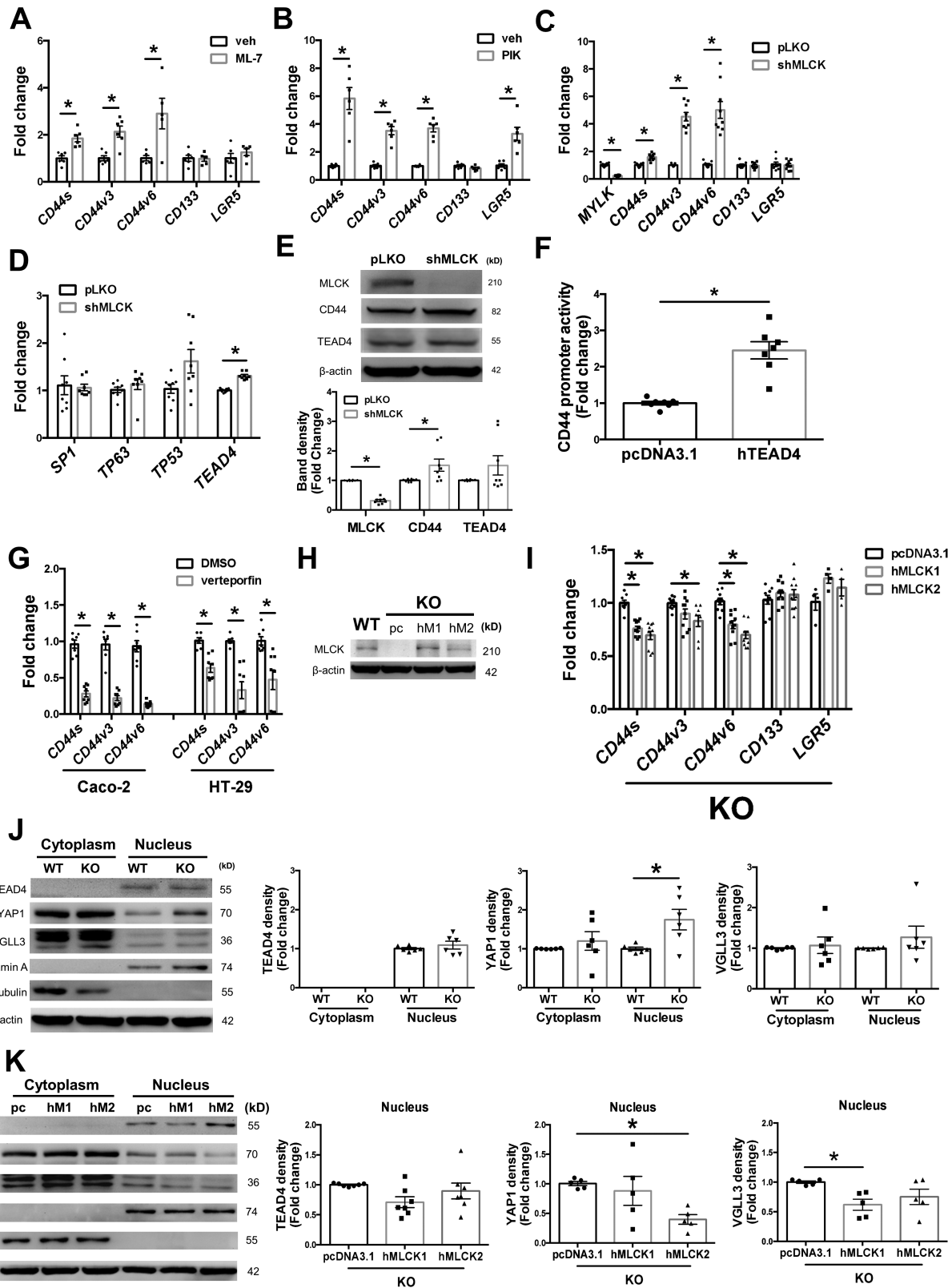


**Figure 5.** MLCK1 and MLCK2 splice variants were involved in the transcriptional repression of CD44 via inhibition of nuclear localization of TEAD4 cofactors, VGLL3 and YAP, respectively. Human Caco-2 cells were treated with pharmacological inhibitors to MLCK or subjected to shRNA-mediated knockdown of MYLK gene. (A) Treatment with ML-7 (20  $\mu$ M, an MLCK inhibitor) for 72 h increased the relative expression of CD44, but not CD133 or LGR5 mRNA. \* $P$  < 0.05 versus vehicle.  $N$  = 6/group. (B) Treatment with PIK (100  $\mu$ M, a specific MLCK inhibitor) for 72 h also increased CD44 mRNA. \* $P$  < 0.05 versus vehicle.  $N$  = 6/group. (C) Gene silencing of MYLK increased the relative expression of CD44, but not CD133 or LGR5 mRNA. \* $P$  < 0.05 versus pLKO.  $N$  = 8–10/group. (D) Knockdown of MYLK gene increased the relative expression of TEAD4 but not other candidate transcription factors.  $N$  = 6/group. \* $P$  < 0.05 versus pLKO.  $N$  = 8–10/group. (E) Western blots and densitometric analysis of MLCK, CD44 and TEAD4 proteins in Caco-2 cells after MYLK gene knockdown.  $N$  = 8/group. \* $P$  < 0.05 versus pLKO. (F) A novel transcriptional factor TEAD4 predicted for binding to CD44 promoter,

available at Carcinogenesis Online). Furthermore, expressing *MLCK2* in the KO cells decreased the nuclear localization of YAP1, whereas expressing *MLCK1* reduced the nuclear localization of VGLL3 (Figure 6B; Supplementary Figure 3, available at Carcinogenesis Online). The results indicated that *MLCK* splice variants regulated the TEAD4 transcriptional activity through distinct coactivators.

### Hyperproliferation in *MLCK* gene KO cells was counterbalanced by the expression of *MLCK1/2* variants

Finally, the roles of *MLCK* splice variants in the regulation of the cell cycle transit were assessed. Cells in the resting quiescent state ( $G_0$  stage) expressed lower levels of Ki67 compared with actively proliferating cells ( $G_1/S/G_2/M$  stages), which have high Ki67 expression. Our results showed a significant elevation of the cell ratio in the  $S/G_2/M$  phases and higher Ki67 intensity in the KO cells than the WT cells (Figure 6C). The faster cell cycle transition was correlated to the increased percentage of cells with high CD44 expression in those KO of *MLCK* gene as evidenced by the flow cytometric dot plot (Figure 6D). A gain-of-function study by individually expressing *MLCK1/2* in the KO cells was next conducted to evaluate which splice variant may reverse the hyperproliferative phenomenon. A reduction in the cell shift to  $S/G_2/M$  phases and decreased Ki67 intensity were observed in the KO cells after expressing *MLCK1* or *MLCK2* (Figure 6E). Based on our results, both *MLCK* splice variants attenuated CD44 expression and reduced tumor proliferation by inhibition of the TEAD4 activity via distinct transcriptional cofactors (Figure 6F).

### Discussion

This study demonstrated that the long isoforms of *MLCK* expressed in intestinal epithelial cells acted as tumor suppressors. Lower levels of *MYLK* and higher *TEAD4/CD44* expression were observed in human CRC, which was confirmed by large-scale bioinformatics analysis. We are the first to provide direct evidence that long *MLCK* restrained malignant transformation of colon epithelia by repressing the TEAD4 transcriptional activity for CD44 expression. Moreover, a previously unreported pathway for divergent control of the transcriptional cofactors VGLL3 and YAP by *MLCK* splice variants was involved in the TEAD4/CD44 axis.

A controversial role of *MLCK* in tumor progression was documented in experimental models despite a consensus of decreased *MLCK* expression in human cancer. Previous work by our laboratory and others demonstrated two splice variants of long *MLCK* in human intestinal epithelial cells (2,3,6). Here, both isoforms of *MLCK* were significantly decreased in the human CRC samples compared with the paired non-tumor tissues and were associated with higher CD44 expression (uncoupled to changes in CD133 or LGR5). Bioinformatics analysis of human sample databases confirmed the low transcript levels of *MYLK* in CRC and the inverse correlation of *MYLK* and CD44 between primary tumors versus normal colonic tissues. We found that approximately 5–6% of CRC patients exhibited *MYLK* gene

mutations in contrast to the low alteration frequency (0–1.5%) of the CD44 gene in cohort studies (43). Although recent reports showed a high abundance of *MYLK* expressed in human lung and colorectal adenocarcinoma as a possible mechanism to compete with classical *MYLK* expression (9,17), no increase of the pseudogene was found in our tumor tissues. Overall, an opposite relationship was found between long *MYLK* and CD44 expression in our tumor samples and by bioinformatics analysis. While our study and others found decreased *MLCK* transcripts in CRC specimens, a recent report showed an increase of *MLCK* expression in hypopharyngeal tumor tissues (44). We observed that downregulated *MLCK* increased the CD44 transcriptional expression in CRC cells, but studies in late-stage colon cancer and hypopharyngeal cancer showed that cell migration and epithelial–mesenchymal transition were dependent on *MLCK* activities (14,15,44). Taken together, epithelial *MLCK* may play multiple roles at different stages of carcinogenesis.

Stem cells constitute only a minor population of the solid tumor mass, but this small subpopulation of colon CSCs expressing CD44 and CD133 was responsible for tumor cell proliferation in a highly efficient manner (45,46). A wide range of percentages of stem-like cells positive of CD44 (11.5–58.4%) and CD133 (0.3–82%) were reported in colon cancers (24). Although the immunoreactivity of CD44 appeared to be higher in some areas of the *MLCK(-/-)* mouse tumors compared with WT, the patchy staining of CD44 in tumor tissues rendered it unable to be quantified. The use of tumor spheroid and crypt organoid culturing allowed the enrichment of stem cells for research. We observed that an increased tumor burden accompanied by higher levels of CD44 but not CD133 or LGR5 in the *MLCK(-/-)* tumorspheres compared with the WT tumorspheres. Consistent with the mouse data, the CD44 protein levels in the *MLCK-KO* cells were increased compared with WT cells by flow cytometric analysis on gated single cells. Interestingly, the CD44, CD133 and LGR5 levels were elevated in colonic organoids derived from the *MLCK(-/-)* mice. LGR5 is a transmembrane receptor for R-spondin binding and when co-stimulated with Wnt ligands, activate  $\beta$ -catenin signaling for cell proliferation. Nevertheless, *in vitro* data demonstrated that modulation of *MLCK* led to transcriptional changes mainly in the CD44 levels (including standard and splice variants) but did not affect other stemness markers. The findings suggested that although LGR5 and CD133 might be associated with higher cell proliferation during the premalignant phase, CD44 was the key player in the response to *MLCK* signals for driving tumor progression.

The standard form and splicing variants of CD44 were implicated in tumor cell proliferation, metastasis and chemoresistance (25,26). Moreover, alternative splicing of CD44 was associated with more advanced stages of colon cancer, and the CD44v4–10 isoforms acted as coreceptors for hepatocyte growth factor and vascular endothelial growth factors (27,47). In our study, the findings of reduced *MYLK* transcripts in human tumors and elevated CD44 expression in mouse colonic organoids with *MLCK* deficiency indicated that the barrier-regulating *MLCK* played a critical role in driving epithelial malignant transformation.

based on GTRD bioinformatics analysis, was identified by luciferase reporter activity. \* $P < 0.05$  versus pcDNA3.1. N = 7/group. (G) Treatment with verteporfin (2  $\mu$ M, an inhibitor to TEAD activity) for 48 h reduced the CD44 transcript levels in Caco-2 and HT-29 cells. N = 6/group. \* $P < 0.05$  versus DMSO. N = 7/group. (H) Representative gel images showing WT Caco-2 cells subjected to CRISPR/Cas9-based KO of *MYLK* gene, and those transfected with pcDNA3.1 (pc) plasmids encoding human *MLCK1* (hM1) or human *MLCK2* (hM2) sequence. The antibodies used for *MLCK* staining cannot distinguish between splice variants. N = 3/group. (I) The KO cells transfected with plasmids encoding hM1 and hM2 were examined for the relative expression of CD44, CD133 and LGR5. \* $P < 0.05$  versus pcDNA3.1. N = 10/group. (J) The presence of TEAD4 transcriptional cofactors YAP1 and VGLL3 in the cytoplasmic and nuclear fractions of cells was examined by Western blotting. \* $P < 0.05$  versus pcDNA3.1. N = 6/group. (K) Representative gel images of the TEAD4, YAP and VGLL3 levels in the KO cells after transfection with pcDNA3.1 or hM1/2-encoding plasmids. Densitometric analysis showing nuclear levels of TEAD4, YAP1 and VGLL3. \* $P < 0.05$  versus pcDNA3.1. N = 5–7/group.

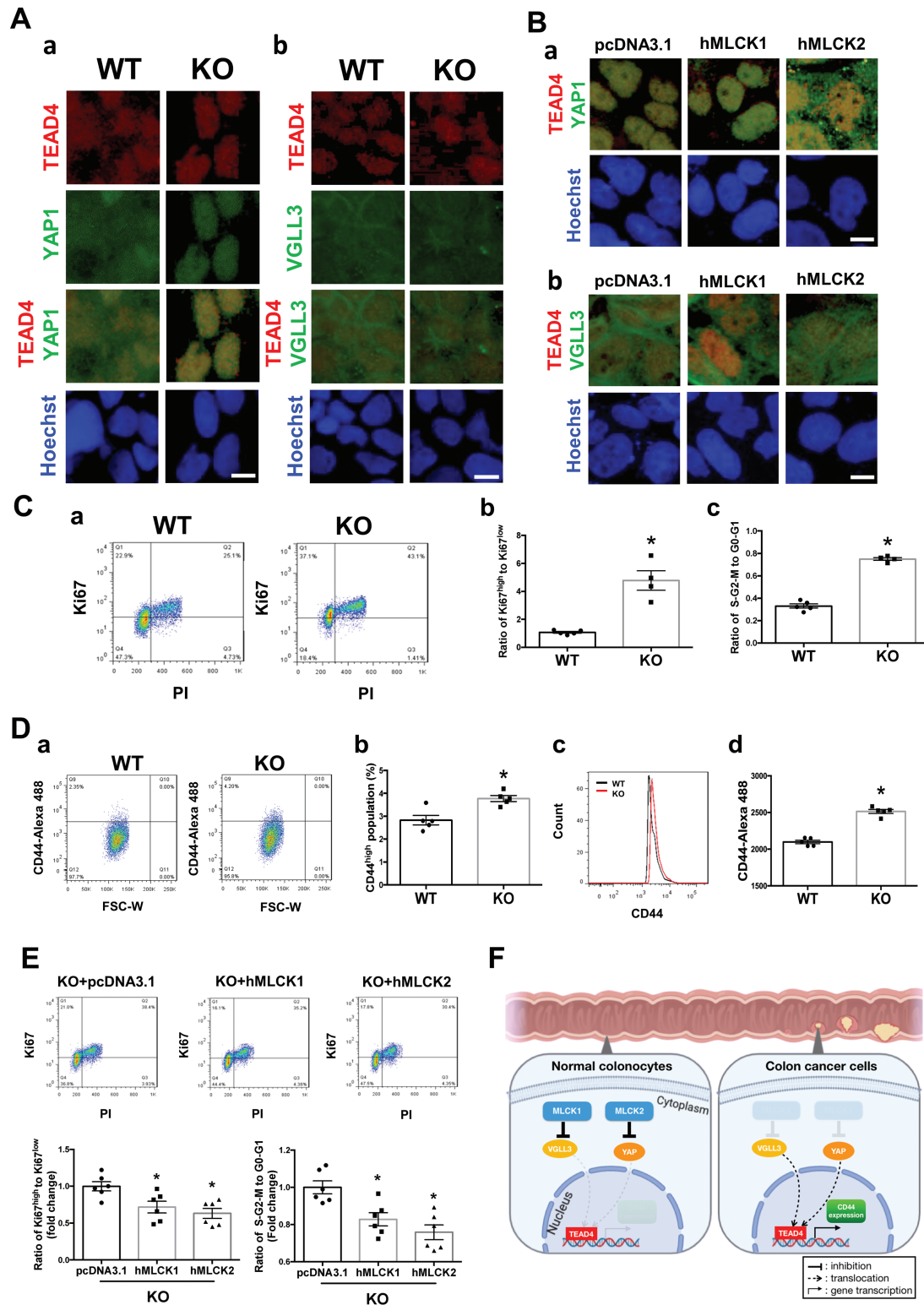


**Figure 6.** Faster cell cycle transit was observed in the MLCK-KO cells, whereas transfection with MLCK1/2-encoding plasmids counterbalanced the cell hyperproliferation. (A) Representative immunofluorescent images of WT and KO cells with double staining of TEAD4 and YAP1 (a) and TEAD4 and VGLL3 (b). The presence of TEAD4 (red) was observed in the cell nuclei (blue) of WT and KO cells by staining with a Hoechst dye. (a) Colocalization of TEAD4 (red) and YAP1 (green) in the cell nuclei and staining of YAP1 in the cytoplasm were found in the WT cells, whereas increased nuclear localization of YAP1 was observed in the KO cells. (b) Cytoplasmic and nuclear staining of VGLL3 (green) was observed in the WT and KO cells, and no difference in the pattern was seen between the two groups. Staining of TEAD4 (red) was found in the cell nuclei (blue). Bar: 10  $\mu$ m. (B) Immunostaining of TEAD4, YAP1 and VGLL3 in the KO cells after transfection with pcDNA3.1 or hMLCK1/2-encoding plasmids. The TEAD4 staining (red) in the cell nuclei (blue) was merged with that of YAP1 (green, a) or VGLL3 (green, b). Decreased nuclear localization of YAP1 was observed in the KO cells expressing hMLCK2, whereas the reduced nuclear presence of VGLL1 was seen by expressing hMLCK1. Bar: 10  $\mu$ m. (C) WT and KO cells were assessed for cell cycle rates by staining with anti-Ki67 and propidium iodide (PI) for flow cytometry. (a) Dot plot of cell cycles. (b) Quantitative results of ratio of high-to-low Ki67. (c) Quantitative

A high level of LGR5 expression (a stem cell marker involved in Wnt/ $\beta$ -catenin signaling) was reported in human tumors (48), but this was not observed in the CRC specimens here. We speculated that specific CRC typing to rule out mesenchymal tumors may yield a more positive result for LGR5 expression in the carcinoma population. Notably, the epithelial chloride-secreting ion channel, cystic fibrosis transmembrane conductance regulator (CFTR), was also recently identified to be tumor suppressors and modulated Wnt/ $\beta$ -catenin signaling (49,50). Further investigation is warranted to determine whether the loss of physiological gene transcription (e.g. MYLK and CFTR) in epithelial cells may initiate tumorigenesis.

Multiple transcription factors for CD44 expression, including SP1, TP63 and TP53, have been previously reported (35–37). We have predicted a novel transcription factor, TEAD4 (a key member of the Hippo pathway), by bioinformatics tools and confirmed its binding to CD44 promoters and the upstream regulation by MLCK. Although human CRC specimens showed a negative correlation of MLCK with all candidate transcription factors (e.g. SP1, TP63, TP53 and TEAD4), large-scale data probing suggested a more cohesive relationship between MLCK and TEAD4 compared with the others. Therefore, it is postulated that the high levels of SP1, TP63 and TP53 in human tumors simply reflect the cancer status with CD44 upregulation, but may not be the consequence of decreased MLCK expression.

Hippo signaling which is an evolutionarily conserved pathway for organ development recently emerged as a key regulator for stemness and oncogenicity (38). The pathway comprises a cascade of kinases and effectors, including YAP/transcriptional coactivator with PDZ-binding motif (TAZ) complex. The nuclear localization of YAP/TAZ pairing with TEAD family members activates the transcription of target genes (38). Recent studies have shown that YAP/TAZ/TEAD4 binds to the SOX2 promoter and promotes cancer stemness and tumorsphere formation in head and neck squamous cell carcinoma (51,52). For studies in colonic epithelia, depletion of YAP/TAZ did not alter normal intestinal homeostasis, but hyperactivation of YAP triggered early onset of polyp formation in colon (39). The VGLL family proteins were recently shown to bind TEAD4 and either compete or cooperate with YAP/TAZ to orchestrate gene transcription (40,41). Tumor cells stably expressing VGLL3 exhibited enhanced proliferation (41), suggesting that VGLL3 was involved in tumor growth. Consistent with our findings, TEAD inhibition was previously shown to diminish cell proliferation and CD44 expression in gastric cancer cells and decreased the pool of tumorsphere-forming CD44-positive gastric CSCs (42).

Our study demonstrated that individual expression of MLCK2 and MLCK1 reduced the nuclear localization of distinct transcriptional cofactors YAP1 and VGLL3 in the TEAD4/CD44 pathway. Although a seemingly redundant function is exerted by the MLCK splice variants for the regulation of tumor stemness, a tight control against malignant transformation may be beneficial for the intestinal organ which is constantly bombarded with infectious agents and noxious foreign substances. Our data are consistent with previous findings of both MLCK splice variants governing the epithelial barrier function, despite separately controlling the paracellular and transcellular permeability

(2,4–6). Considering the tissue compartmentation of MLCK splice variants—MLCK2 on epithelial cells spanning the crypt to villus region and higher MLCK1 expression on differentiated surface epithelia (2,4), it is possible that both the crypt MLCK2/YAP1 and surface epithelial MLCK1/VGLL3 pathways are acting to inhibit CD44 stemness, which coincides with the bottom-up and top-down model of cancer origin. A larger drop in the transcript levels of MLCK2 than MLCK1 was observed in the clinical tumor specimens. The *in vitro* data also showed a 2-fold increase in the nuclear YAP1 levels but no change in the nuclear VGLL3 levels after KO of all MLCK splice variants in human CRC cell lines, implicating that MLCK2 played a more dominant role than MLCK1 for suppression of CD44 transcription. Although VGLL3 has been traditionally considered a transcriptional cofactor located in the nucleus, we observed immunoreactivity to VGLL3 not only in the nucleus but also as strand-like cytoskeletal patterns in the cellular cytoplasm which was not extracted by detergent in the cytoplasmic fraction for western blotting. Recent articles also suggested that VGLL3 was involved in actin cytoskeleton regulation and myofibril differentiation (53,54). This finding implicated that in addition to MLCK-mediated regulation of nuclear VGLL3–TEAD4 interaction, there may be other unknown biological functions of cytoplasmic VGLL3. Whether human tumors at different stages display loss of distinct MLCK variants and its pathological significance regarding a dysregulated Hippo pathways warrant further investigation.

In conclusion, long MLCK downregulated CD44 expression via inhibition of TEAD4 transcriptional activity in intestinal epithelial cells. Our study is the first to show that MLCK splice variants 1/2, beyond divergent control of gut barrier functions, serve as tumor suppressors by restraining the TEAD4/CD44 axis via distinct transcriptional cofactors VGLL3 and YAP1. The reduction of epithelial MLCK, especially isoform 2, may drive cancer stemness and tumorigenesis.

## Supplementary material

Supplementary data are available at *Carcinogenesis* online.

**Supplementary Figure 1.** Deficiency of MYLK gene was confirmed on colonic tissues of MLCK(–/–) mice. (A) Deletion of MYLK gene in the long MLCK(–/–) mice was confirmed by PCR on colonic mucosal tissues. A neomycin-resistant gene was inserted into MLCK exon 8 to disrupt protein translation in MLCK(–/–) mice. (B) Normal morphology of colonic tissues was observed in untreated MLCK(–/–) and WT B6 mice. Magnification:  $\times 200$ .

**Supplementary Figure 2.** Overexpression of MLCK splice variants in Caco-2 cells reduced CD44 transcript levels. (A) WT Caco-2 cells were transfected with pcDNA3.1 plasmids encoding human MLCK splice variants (hMLCK1 and hMLCK2). Transfection efficiency of (a) MLCK1 and (b) MLCK2 was confirmed by quantitative PCR in the WT Caco-2 cells. \* $P < 0.05$  versus pcDNA3.1.  $N = 4$ /group. (B) Transcript levels of CD44, CD133 and LGR5 in WT cells overexpressing MLCK1/2. \* $P < 0.05$  versus pcDNA3.1.  $N = 6$ /group. (C) Caco-2 cells subjected to CRISPR/Cas9-based KO of MYLK gene were transfected with pcDNA3.1 plasmids encoding human MLCK splice variants (hMLCK1 and hMLCK2). Transfection efficiency of (a) MLCK1 and (b) MLCK2 was confirmed by quantitative

results of ratio of S–G<sub>2</sub>–M to G<sub>0</sub>–G<sub>1</sub> phases.  $N = 4$ –5/group. \* $P < 0.05$  versus WT. Experiments were repeated at least twice. (D) CD44 expression in WT and KO cells. (a) Dot plot of CD44 staining. (b) Percentages of cells with high CD44 intensity. (c and d) Histogram and mean intensity of CD44 staining in the top 10% cell population with high expression.  $N = 5$ /group. \* $P < 0.05$  versus WT. (E) The KO cells transfected with plasmids encoding hMLCK1 or hMLCK2 exhibited a decrease in cell cycle rates.  $N = 6$ /group. \* $P < 0.05$  versus pcDNA3.1. (F) Schematic diagram of long MLCK-mediated suppression of CD44 gene transcription and tumor cell proliferation. Constitutive expression of long MLCK inhibited the TEAD4 transcriptional activity in normal colonocytes, whereas reduced expression of MLCK1 and MLCK2 splice variants in cancer cells led to enhanced nuclear translocation of the TEAD4 transcriptional cofactors, VGLL3 and YAP1, respectively, and increased the CD44 gene expression.

PCR in the KO cells. \* $P < 0.05$  versus pcDNA3.1.  $N = 8/\text{group}$ . (D) Sequencing of the MYLK gene in WT cells and those subjected to KO using the CRISPR/Cas9 gene editing system. The label ATG indicates the start codon of the human MYLK gene. The first and second targeting sites of CRISPR (CR) RNA binding sequences denoted CR1 and CR2 were designed before and after the start codon of MYLK gene. Lack of consensus (lower case letters in blue colors or dots) in the nucleotide sequence from CR1 to CR2 sites was observed between the WT and KO cells. The absence of MLCK protein in the KO cells was confirmed by western blots in Figure 5H.

**Supplementary Figure 3.** Immunofluorescent staining of TEAD4 and its transcriptional cofactors YAP1 and VGLL3 in cells. Representative immunofluorescent images of KO cells transfected with pcDNA3.1 or hMLCK1/2-encoding plasmids. Photoimages showing double staining of TEAD4 and YAP1 (a) and double staining of TEAD4 and VGLL3 (b). The TEAD4 staining (red) in the cell nuclei (blue) was merged with that of YAP1 (green, a) or VGLL3 (green, b). The staining of cell nucleus by a Hoechst dye was displayed to show cell orientation. Decreased nuclear localization of YAP1 was observed in the KO cells expressing hMLCK2, whereas the reduced nuclear presence of VGLL1 was seen by expressing hMLCK1. Bar: 10  $\mu\text{m}$ .

**Supplementary Table 1.** Characteristics of patients with colorectal cancers

**Supplementary Table 2.** Primer pairs of quantitative PCR for human cells

**Supplementary Table 3.** Primer pairs of quantitative PCR for mouse cells

**Supplementary Table 4.** Primer pairs of reverse transcription PCR for human cells

## Funding

This study was supported by grants from the Ministry of Science and Technology (MOST 107-2320-B-002-041-MY3, 106-2320-B-002-017, 104-2320-B-002-008-MY3, 106-2813-C-002-115-B), National Health Research Institute (NHRI-EX108-10823BI, NHRI-EX109-10823BI, NHRI-EX110-10823BI) and National Taiwan University (NTU-CDP-105R7798, NTU-CCP-106R890504, NTU-CC-109L893102) to L.C.-H.Y., and National Institutes of Health (R01-DK068271) to J.R.T.

**Conflict of Interest Statement:** The authors declare that there is no conflict of interest.

## References

- Lazar, V. et al. (1999) A single human myosin light chain kinase gene (MLCK; MYLK). *Genomics*, 57, 256–267.
- Clayburgh, D.R. et al. (2004) A differentiation-dependent splice variant of myosin light chain kinase, MLCK1, regulates epithelial tight junction permeability. *J. Biol. Chem.*, 279, 55506–55513.
- Blair, S.A. et al. (2006) Epithelial myosin light chain kinase expression and activity are upregulated in inflammatory bowel disease. *Lab. Invest.*, 86, 191–201.
- Graham, W.V. et al. (2019) Intracellular MLCK1 diversion reverses barrier loss to restore mucosal homeostasis. *Nat. Med.*, 25, 690–700.
- Wu, L.L. et al. (2014) Commensal bacterial endocytosis in epithelial cells is dependent on myosin light chain kinase-activated brush border fanning by interferon- $\gamma$ . *Am. J. Pathol.*, 184, 2260–2274.
- Pai YC. et al. (2021) Gut microbial transcytosis induced by tumor necrosis factor-like 1A-dependent activation of a myosin light chain kinase splice variant contributes to IBD. *J. Crohns Colitis*, 15, 258–272.
- Bray, F. et al. (2018) Global cancer statistics 2018: GLOBOCAN estimates of incidence and mortality worldwide for 36 cancers in 185 countries. *CA. Cancer J. Clin.*, 68, 394–424.
- Lee, W.S. et al. (2008) Identification of differentially expressed genes in microsatellite stable HNPCC and sporadic colon cancer. *J. Surg. Res.*, 144, 29–35.
- Han, Y.J. et al. (2011) A transcribed pseudogene of MYLK promotes cell proliferation. *FASEB J.*, 25, 2305–2312.
- Suzuki, M. et al. (2014) Myosin light chain kinase expression induced via tumor necrosis factor receptor 2 signaling in the epithelial cells regulates the development of colitis-associated carcinogenesis. *PLoS One*, 9, e88369.
- Gu, L.Z. et al. (2006) Inhibiting myosin light chain kinase retards the growth of mammary and prostate cancer cells. *Eur. J. Cancer*, 42, 948–957.
- Dulyaninova, N.G. et al. (2004) The N-terminus of the long MLCK induces a disruption in normal spindle morphology and metaphase arrest. *J. Cell Sci.*, 117(Pt 8), 1481–1493.
- Wu, Q. et al. (2010) Deficiency in myosin light-chain phosphorylation causes cytokinesis failure and multipolarity in cancer cells. *Oncogene*, 29, 4183–4193.
- Avizienyte, E. et al. (2005) The SRC-induced mesenchymal state in late-stage colon cancer cells. *Cells Tissues Organs*, 179, 73–80.
- Zuo, L. et al. (2016) All-trans retinoic acid inhibits human colorectal cancer cells RKO migration via downregulating myosin light chain kinase expression through MAPK signaling pathway. *Nutr. Cancer*, 68, 1225–1233.
- Zhang, L. et al. (2018) Fenretinide inhibits the proliferation and migration of human liver cancer HepG2 cells by downregulating the activation of myosin light chain kinase through the p38-MAPK signaling pathway. *Oncol. Rep.*, 40, 518–526.
- Lynn, H. et al. (2018) Single nucleotide polymorphisms in the MYLK1 pseudogene are associated with increased colon cancer risk in African Americans. *PLoS One*, 13, e0200916.
- Papailiou, J. et al. (2011) Stem cells in colon cancer. A new era in cancer theory begins. *Int. J. Colorectal Dis.*, 26, 1–11.
- Todaró, M. et al. (2010) Colon cancer stem cells: promise of targeted therapy. *Gastroenterology*, 138, 2151–2162.
- Najafi, M. et al. (2019) Cancer stem cells (CSCs) in cancer progression and therapy. *J. Cell. Physiol.*, 234, 8381–8395.
- Thapa, R. et al. (2016) The importance of CD44 as a stem cell biomarker and therapeutic target in cancer. *Stem Cells Int.*, 2016, 2087204.
- Chen, K.L. et al. (2011) Highly enriched CD133<sup>+</sup>CD44<sup>+</sup> stem-like cells with CD133<sup>+</sup>CD44<sup>high</sup> metastatic subset in HCT116 colon cancer cells. *Clin. Exp. Metastasis*, 28, 751–763.
- Zhou, J.Y. et al. (2016) Role of CD44<sup>high</sup>/CD133<sup>high</sup> HCT-116 cells in the tumorigenesis of colon cancer. *Oncotarget*, 7, 7657–7666.
- Haraguchi, N. et al. (2008) CD133<sup>+</sup>CD44<sup>+</sup> population efficiently enriches colon cancer initiating cells. *Ann. Surg. Oncol.*, 15, 2927–2933.
- Ma, L. et al. (2019) CD44v6 engages in colorectal cancer progression. *Cell Death Dis.*, 10, 30.
- Sakuma, K. et al. (2018) HNRNPLL, a newly identified colorectal cancer metastasis suppressor, modulates alternative splicing of CD44 during epithelial-mesenchymal transition. *Gut*, 67, 1103–1111.
- Joosten, S.P.J. et al. (2017) MET signaling mediates intestinal crypt-villus development, regeneration, and adenoma formation and is promoted by Stem Cell CD44 Isoforms. *Gastroenterology*, 153, 1040–1053.e4.
- Huang, C.Y. et al. (2019) Glucose metabolites exert opposing roles in Tumor Chemoresistance. *Front. Oncol.*, 9, 1282.
- Owens, S.E. et al. (2005) A strategy to identify stable membrane-permeant peptide inhibitors of myosin light chain kinase. *Pharm. Res.*, 22, 703–709.
- Kuo, W.T. et al. (2015) LPS receptor subunits have antagonistic roles in epithelial apoptosis and colonic carcinogenesis. *Cell Death Differ.*, 22, 1590–1604.
- Kuo, W.T. et al. (2016) Eritoran suppresses colon cancer by altering a functional balance in toll-like receptors that bind lipopolysaccharide. *Cancer Res.*, 76, 4684–4695.
- Lee, T.C. et al. (2018) Hypoxia-induced intestinal barrier changes in balloon-assisted enteroscopy. *J. Physiol.*, 596, 3411–3424.
- Huang, C.Y. et al. (2020) Distinct patterns of interleukin-12/23 and tumor necrosis factor  $\alpha$  synthesis by activated macrophages are modulated by glucose and colon cancer metabolites. *Chin. J. Physiol.*, 63, 7–14.

34. Wu, L.L. et al. (2011) Epithelial inducible nitric oxide synthase causes bacterial translocation by impairment of enterocytic tight junctions via intracellular signals of Rho-associated kinase and protein kinase C zeta. *Crit. Care Med.*, 39, 2087–2098.
35. Luo, Y. et al. (2020) Isorhapontigenin (ISO) inhibits stem cell-like properties and invasion of bladder cancer cell by attenuating CD44 expression. *Cell. Mol. Life Sci.*, 77, 351–363.
36. Boldrup, L. et al. (2007) ΔNp63 isoforms regulate CD44 and keratins 4, 6, 14 and 19 in squamous cell carcinoma of head and neck. *J. Pathol.*, 213, 384–391.
37. Godar, S. et al. (2008) Growth-inhibitory and tumor-suppressive functions of p53 depend on its repression of CD44 expression. *Cell*, 134, 62–73.
38. Misra, J.R. et al. (2018) The Hippo signaling network and its biological functions. *Annu. Rev. Genet.*, 52, 65–87.
39. Cai, J. et al. (2010) The Hippo signaling pathway restricts the oncogenic potential of an intestinal regeneration program. *Genes Dev.*, 24, 2383–2388.
40. Figeac N. et al. (2019) VGLL3 operates via TEAD1, TEAD3 and TEAD4 to influence myogenesis in skeletal muscle. *J. Cell Sci.*, 132, jcs225946.
41. Hori, N. et al. (2020) Vestigial-like family member 3 (VGLL3), a cofactor for TEAD transcription factors, promotes cancer cell proliferation by activating the Hippo pathway. *J. Biol. Chem.*, 295, 8798–8807.
42. Giraud, J. et al. (2020) Verteporfin targeting YAP1/TAZ-TEAD transcriptional activity inhibits the tumorigenic properties of gastric cancer stem cells. *Int. J. Cancer*, 146, 2255–2267.
43. Xia, P. et al. (2016) Prognostic significance of CD44 in human colon cancer and gastric cancer: evidence from bioinformatic analyses. *Oncotarget*, 7, 45538–45546.
44. Cao, F. et al. (2020) Myosin light chain kinase is a potential target for hypopharyngeal cancer treatment. *Biomed. Pharmacother.*, 131, 110665.
45. Wang, D. et al. (2015) Prostaglandin E2 promotes colorectal cancer stem cell expansion and metastasis in mice. *Gastroenterology*, 149, 1884–1895.e4.
46. Dalerba, P. et al. (2007) Phenotypic characterization of human colorectal cancer stem cells. *Proc. Natl. Acad. Sci. USA*, 104, 10158–10163.
47. Volz Y. et al. (2015) Direct binding of hepatocyte growth factor and vascular endothelial growth factor to CD44v6. *Biosci. Rep.*, 35, e00236.
48. Shimokawa, M. et al. (2017) Visualization and targeting of LGR5<sup>+</sup> human colon cancer stem cells. *Nature*, 545, 187–192.
49. Than, B.L. et al. (2016) CFTR is a tumor suppressor gene in murine and human intestinal cancer. *Oncogene*, 35, 4179–4187.
50. Strubberg, A.M. et al. (2018) Cftr modulates Wnt/β-catenin signaling and stem cell proliferation in murine intestine. *Cell. Mol. Gastroenterol. Hepatol.*, 5, 253–271.
51. Li, J. et al. (2019) The Hippo effector TAZ promotes cancer stemness by transcriptional activation of SOX2 in head neck squamous cell carcinoma. *Cell Death Dis.*, 10, 603.
52. Bora-Singhal, N. et al. (2015) YAP1 regulates OCT4 activity and SOX2 expression to facilitate self-renewal and vascular mimicry of stem-like cells. *Stem Cells*, 33, 1705–1718.
53. Kurko, J. et al. (2020) Transcription profiles of age-at-maturity-associated genes suggest cell fate commitment regulation as a key factor in the Atlantic salmon maturation process. *G3 (Bethesda)*, 10, 235–246.
54. Gabay Yehezkely, R. et al. (2020) Intracellular role for the matrix-modifying enzyme lox in regulating transcription factor subcellular localization and activity in muscle regeneration. *Dev. Cell*, 53, 406–417.e5.